Chemical Engineering Journal 157 (2010) 297–303

Contents lists available at ScienceDirect

Chemical Engineering Journal

journal homepage: www.elsevier.com/locate/cej

Novel simulation model of the solar collector of BIOCOIL photobioreactors for CO_2 sequestration with microalgae

Alessandro Concas[a], Massimo Pisu[a], Giacomo Cao[a,b,c,*]

[a] CRS4, Center for Advanced Studies, Research and Development in Sardinia, Parco Scientifico e Tecnologico, Edificio 1, 09010 Pula, CA, Italy
[b] Dipartimento di Ingegneria Chimica e Materiali, Unità di Ricerca del Consorzio Interuniversitario Nazionale "La Chimica per l'Ambiente" (INCA), Unità di Ricerca del Dipartimento Energia e Trasporti del Consiglio Nazionale delle Ricerche, Piazza d'Armi, 09123 Cagliari, Italy
[c] Centro Interdipartimentale di Ingegneria e Scienze Ambientali, Laboratorio di Cagliari del Consorzio INCA, Via San Giorgio 12, 09124 Cagliari, Italy

ARTICLE INFO

Article history:
Received 6 August 2009
Received in revised form 26 October 2009
Accepted 27 October 2009

Keywords:
Microalgae
Photobioreactors
BIOCOIL
CO_2 sequestration
Mathematical modeling
Population balance

ABSTRACT

A novel mathematical model to simulate the growth of microalgae in the solar collector of recirculating helical photobioreactors (BIOCOIL) is proposed. The dynamic-spatial behavior of the nutrient species in liquid phase (CO_2, nitrates and orthophosphates) and the primary photosynthesis product (O_2) are quantitatively described through the proposed model where the simulation of cell growth, proliferation and its distribution within the tubular section of the helical photobioreactor is improved with respect to the existing literature by properly taking into account suitable population balances. Light intensity distribution within the culture medium is also quantitatively described. Model results and the literature experimental data in terms of dry biomass content and its distribution within the photobioreactor tube have been successfully compared, thus demonstrating the validity of the proposed model as well as its predictive capability.

1. Introduction

The production of biofuels from algal biomass is one of the most ambitious task to fulfill a sustainable ecological balance worldwide. The main goal is the reduction of environmental contamination by recycling part of the CO_2 produced through energy generation by fossil fuels and use it to obtain biofuels or other valuable products. Recently, the possibility of employing photoautotrophic microalgae that utilize CO_2 as a carbon source for their growth, and the subsequent production of biofuels or other valuable products from the obtained algal biomass, has been investigated [1,2].

The proposed processes are based on the use of specific photobioreactors where different types of algae are cultivated using suitable nutrients as well as CO_2 as carbon source.

A variety of photobioreactors have been proposed in the literature [1,3–5]. Reactor configurations vary from horizontal tubular systems [6] to helical tubular reactors [7,8], cascade reactors [9], alveolar flat panels [10] and others, as reported by [11].

Horizontal or helical tubular systems, as well as combinations of vertical flat panels and bubble columns appear to be the reactor configurations whose scale up may be relatively straightforward [11]. In particular, the patented helical configuration named BIOCOIL is characterized by very simple and relatively inexpensive design, easy to assemble and operate. Moreover, small space requirement as compared to other equipments is required by BIOCOIL reactors. It has been recently recognized that the development and application of the technology for CO_2 sequestration based on photobioreactors needs to be optimized from the operational point of view in terms of selected algal species, sunlight, temperature as well as the corresponding design parameters, i.e. light regime, heat and mass transfer conditions, etc. [11]. In addition, such technology has not been easily scaled-up since experimental data from laboratory reactors have not been correctly interpreted [12].

To this aim, suitable mathematical models of photobioreactors have been proposed. So far, the basic characteristics of algal kinetics [13–23] have been taken into account.

Most mathematical models available in the literature were also capable of quantitatively describing light distribution within the culture [13,14]. However, only few of them were devoted to predict biomass, dissolved oxygen and carbon dioxide concentration profiles in tubular photobioreactors [18], pH evolution [22], mass transfer [16] and the influence of hydrodynamic regime on light conversion [23]. Recently, Wu and Merchuk [19] proposed a dynamic model which accounts for photosynthesis and

* Corresponding author at: Dipartimento di Ingegneria Chimica e Materiali, Unità di Ricerca del Consorzio Interuniversitario Nazionale "La Chimica per l'Ambiente" (INCA), Unità di Ricerca del Dipartimento Energia e Trasporti del Consiglio Nazionale delle Ricerche, Piazza d'Armi, 09123 Cagliari, Italy. Tel.: +39 070 675 50 58; fax: +39 070 675 50 57.
E-mail address: cao@visnu.dicm.unica.it (G. Cao).

1385-8947/$ – see front matter © 2009 Elsevier B.V. All rights reserved.
doi:10.1016/j.cej.2009.10.059

photoinhibition phenomena on the basis of the three states model of photosynthetic factories (PSF), originally proposed by Eilers and Peeters [24].

To the best of our knowledge, despite the large number of mathematical models appearing in the literature to simulate photobioreactors, no comprehensive models, which accounts for all complex phenomena taking place, including algal cell metabolism as well as microalgae population, have been proposed. Most of these models are based upon the assumption that individual cells have the same growth rate, biochemical composition and metabolism. On the other hand, the latter ones are strongly related to the cell size or cell mass [25–27]. In particular, smaller algae achieve higher rates of photosynthesis, have higher specific growth rates and also a faster uptake of nutrients per unit of biomass [28]. Since an algae population is a system where algae of different sizes are present, the assumption that all cells have the same dimension or mass may determine significant errors when simulating the behavior of an algal culture within a photobioreactor. In fact, cells having different size or mass will be erroneously described as if characterized by the same growth rate. Moreover, the correct simulation of algae size distribution will also provide appropriate insights with respect to operational photobioreactor parameters. In fact, during typical algal cultivation processes, a suitable harvesting step using suitable centrifuges is required because cells are stabilized and suspended in broth due to their small size, low concentration and electrical stability. Accordingly, they do not settle out of the broth due to gravity in realistic time frame [29]. Consequently, if the dispersed algal cells are characterized by large average diameters, phenomena such autoflocculation could take place so that microalgae could be more easily separated through a simple gravitational settling operation thus allowing a cost-effective harvesting of microalgae.

For these reasons, the quantitative description of the evolution of cell size distribution during microalgae cultivation cannot be missed when developing suitable mathematical models of microalgae growth within photobioreactors.

In the present work we propose a simulation model to quantitatively describe the growth of microalgae in the tubular section of recirculating helical photobioreactors (BIOCOIL). The model accounts for "mass structured" population balances which permit to properly simulate cell growth, replication and its distribution within the tubular-helical photobioreactor. Specifically, a novel mass-dependent growth kinetics has been proposed. The latter one takes also into account light intensity, nutrients concentration and inhibitory effects of dissolved oxygen. Light intensity distribution within the culture medium is also accounted for. Model results and the literature experimental data [30] in terms of dry biomass content and its distribution within the photobioreactor tube have been successfully compared, thus demonstrating the validity of the proposed model as well as its predictive capability.

2. Mathematical modeling

The BIOCOIL photobioreactor, schematically illustrated in Fig. 1, consists of several sections of PVC tubing that is wound horizontally around a vertical, cylindrical wire frame. It may be illuminated either by sunlight or fluorescent lights. Microalgal cells are suspended in a liquid medium (broth) where all nutrients, such as nitrates, phosphates and others, are previously dissolved. Liquid circulation is assured by an airlift where the flue gas containing CO_2 is bubbled in the broth thus allowing the uplifting of the liquid.

According to the original work from which the experimental data are taken [30], the continuous supply of carbon dioxide in the airlift avoids carbon starvation during microalgal growth [17]. Other nutrients are effectively integrated only after 1.81×10^6 s

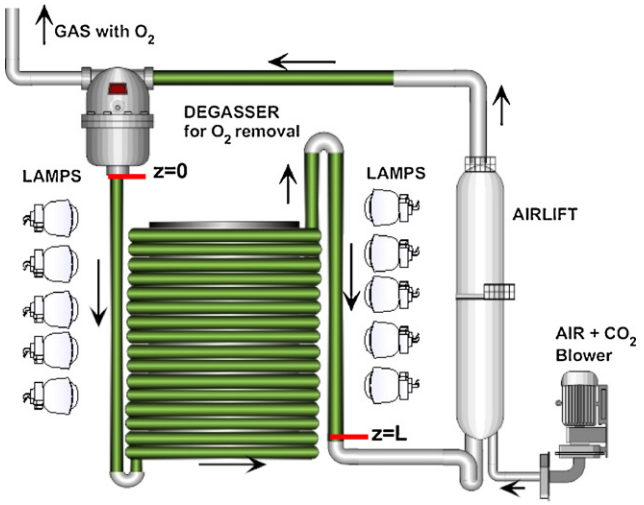

Fig. 1. Schematic representation of BIOCOIL photobioreactor.

(about 21 days), when their stepwise replacement is started and maintained up to 40 days of algae cultivation.

The approach to simulate the growth of microalgae in the tubular section of the photobioreactor is based upon the classical homogeneous, isothermal, axial dispersion model for main nutrient species (C, N, P) and photosynthesis product (O_2) present in the liquid phase. Specifically, the phenomena taking place in the airlift are neglected, since only the tubular section of the experimental apparatus is modeled. It is worth noting that microalgae may use as carbon source the dissolved CO_2, HCO_3^- and CO_3^{2-} that are available within the liquid medium. Since experimental data [30] were obtained from trials where concentration of HCO_3^- and CO_3^{2-} dissolved in the broth were very high and the consumed carbon was reintegrated by CO_2 dissolution in the airlift system, carbon was not considered as limiting nutrient in our model. Furthermore, we assume that photosynthetic O_2 is removed within the degasser by means of stripping procedures, so that the liquid re-circulated in the tubular stage (light collector) contains O_2 concentration close to the saturation value in water. For the reasons above the presence of gas in the tubular section is neglected. Under these assumptions, and considering the tubular geometry of the photobioreactor, the relevant material balances of our model may be written as follows:

$$\frac{\partial C_j}{\partial t} = -v_z \cdot \frac{\partial C_j}{\partial z} + E_D \cdot \frac{\partial^2 C_j}{\partial z^2} - \frac{1}{y_{X/j}} \int_0^\infty \zeta_m(m, z, I, C_j, C_{O_2}) \cdot \psi(m, z) \cdot dm \quad (1)$$

$j = 1,\ 2; \quad 1 = NO_3^-; \quad 2 = H_2PO_4^-$

along with the following initial and boundary conditions:

$$C_j = C_j^0 \qquad @\, t = 0, \forall z \in [0, L] \quad \text{for } j = 1, 2 \quad (2)$$

$$v_z C_j\big|_{z=0^-} = v_z C_j\big|_{z=0^+} - E_D \left.\frac{\partial C_j}{\partial z}\right|_{z=0^+} \qquad @\, z = 0, \forall t > 0 \ \text{ for } j = 1, 2 \quad (3)$$

$$\left.\frac{\partial C_j}{\partial z}\right|_{z=L} = 0 \qquad @\, z = L, \forall t > 0 \quad \text{for } j = 1, 2 \quad (4)$$

It should be noted that in the classical Danckwerts' boundary condition given by Eq. (3) $C_j\big|_{z=0^-} = C_j\big|_{z=L}$, since nutrients are completely re-circulated from the outlet ($z = L$) to the inlet section ($z = 0$)

of the photobioreactor. The material balance for oxygen may be expressed as follows:

$$\frac{\partial C_{O_2}}{\partial t} = -v_z \cdot \frac{\partial C_{O_2}}{\partial z} + E_D \cdot \frac{\partial^2 C_{O_2}}{\partial z^2} + \frac{1}{y_{X/O_2}} \int_0^\infty \zeta_m(m, z, I, C_j, C_{O_2}) \cdot \psi(m, z) \cdot dm \quad (5)$$

along with the following initial and boundary conditions:

$$C_{O_2} = C^0_{O_2} \qquad @\, t = 0, \forall z \in [0, L] \quad (6)$$

$$v_z C_{O_2}\big|_{z=0^-} = v_z C_{O_2}\big|_{z=0^+} - E_D \frac{\partial C_{O_2}}{\partial z}\bigg|_{z=0^+} \qquad @\, z = 0, \forall t > 0 \quad (7)$$

$$\frac{\partial C_{O_2}}{\partial z}\bigg|_{z=L} = 0 \qquad @\, z = L, \forall t > 0 \quad (8)$$

where the symbol significance is reported in Section 5. As discussed above, oxygen is not re-circulated in order to avoid inhibitory effects on algal growth. Since in the simulated experimental trials considered in this work [30] the degassing operation is performed by means of stripping procedures, it is assumed that, at the degasser outlet and thus at the inlet section ($z = 0$) of the loop, oxygen concentration is equal to the saturation concentration of oxygen in water (i.e. $C^0_{O_2} = 9.1\ \mathrm{mg\,L^{-1}}$), so that $C_{O_2}\big|_{z=0^-} = C^0_{O_2}$.

The nutrients, i.e. NO_3^- and $H_2PO_4^-$, are, instead, recirculated at the photobioreactors inlet. In the reactive term of Eqs. (1) and (5), the time rate of change of the mass m for a single microalgal cell, ζ_m may be expressed [31] according to the Monod's model for multiple nutrient limitation [32] where cell mass, concentration of limiting nutrients, photosynthetically active radiation as well as dissolved oxygen concentration are accounted for. Specifically, by considering the equation proposed by Molina et al. [6], being the inhibitory effect of dissolved oxygen taken from Li et al. [21], the following expression of the time rate of change of cell mass is used in the proposed model:

$$\zeta_m(m, z, I, C_j, C_{O_2}) = \left[\mu_{\max} \cdot \frac{I^n}{I_K^n + I^n} \cdot \prod_{j=1}^{2} \frac{C_j}{K_j + C_j} \cdot \left(1 - \frac{C_{O_2}}{C_{O_2,\max}}\right) - \mu_c \right] \cdot m \quad (9)$$

where the symbol significance is reported in Section 5. It should be noted that μ_c is the catabolic rate constant which, due to the lack of information available in the literature, has been assumed equal to zero during the simulations.

To evaluate the biomass concentration, the following "mass structured" population balance [32] is taken into account:

$$\frac{\partial \psi}{\partial t} + \frac{\partial(\zeta_m \cdot \psi)}{\partial m} = -v_z \cdot \frac{\partial \psi}{\partial z} + E_D \cdot \frac{\partial^2 \psi}{\partial z^2} + \Gamma(m, z, I, C_j, C_{O_2}) \cdot \psi - 2 \int_m^\infty \psi \cdot \Gamma(m', z, I, C_j, C_{O_2}) \cdot p(m, m') \cdot dm' \quad (10)$$

along with the following initial and boundary conditions:

$$\psi(m, z, t) = \psi^0(m, z, 0) \qquad @\, t = 0,\ \forall z \in [0, L] \quad (11)$$

$$v_z \cdot \psi\big|_{z=0^-} = v_z \cdot \psi\big|_{z=0^+} - E_D \cdot \frac{\partial \psi}{\partial z}\bigg|_{z=0^+} \qquad @\, z = 0, \forall t > 0 \quad (12)$$

$$\frac{\partial \psi}{\partial z}\bigg|_{z=L} = 0 \qquad @\, z = L, \forall t > 0 \quad (13)$$

where Ψ represents the cell mass distribution while the remaining symbol significance is reported in Section 5.

In Eq. (10) the two terms of the left-hand-side represent the accumulation and the cell growth term, respectively. On the other hand, the first two terms of the right-hand-side of Eq. (10) represent the convective and dispersive terms while the third one is related to the death of mother cell due to mitosis. Finally, the fourth term of the right-hand-side of Eq. (10), represents the cell birth by mitosis where two daughters cells are obtained from one mother cell. It should be noted that in the classical Danckwerts' boundary condition given by Eq. (12), $\psi\big|_{z=0^-} = \psi\big|_{z=L}$, since biomass is completely recirculated from the outlet ($z = L$) to the inlet section ($z = 0$) of the photobioreactor.

The fraction (Γ) of dividing cells of mass m', and the probability partition function for dividing cells (p) may be expressed as follows [31]:

$$\Gamma(m, z, I, C_j, C_{O_2}) = \zeta_m(m, z, I, C_j, C_{O_2}) \cdot \frac{1/\sqrt{2\pi\sigma^2}\exp[-(m-\mu_0)^2/2\sigma^2]}{1 - \int_0^m \frac{1}{\sqrt{2\pi\sigma^2}} \exp -(m'-\mu_0)^2/2\sigma^2 \cdot dm'} \quad (14)$$

$$p(m, m') = \frac{1}{\beta(q, q)} \frac{1}{m'} \left(\frac{m}{m'}\right)^{q-1} \left(1 - \frac{m}{m'}\right)^{q-1} \quad (15)$$

where σ and μ_0 are the standard deviation and the average cellular mass of dividing cells of the division probability density function, respectively, while $\beta(q,q)$ is the symmetric beta function. Γ is also called the division intensity function and represents the tendency of the budding cells to divide as they approach a certain critical mass μ_0. The probability partition function p describes the mass distribution of newborn daughter cells resulting form mother cell division being:

$$\int_0^m p(m, m') \cdot dm' = 1 \quad (15b)$$

The local biomass concentration X, is then evaluated as the first moment of the population through the following expression:

$$X(t, z) = \int_0^\infty \psi(m, z) \cdot m \cdot dm \quad (16)$$

The average light intensity I within the culture in tubular photobioreactors may be expressed as follows [20]:

$$I = I(t, z) = \frac{I_0(t)}{\phi_{eq} K_a X(t, z)} \cdot [1 - \exp(-\phi_{eq} K_a X(t, z))] \quad (17)$$

where ϕ_{eq} is the length of light path that is related with the tube diameter, K_a is the optical extinction coefficient for biomass, and I_0 is the incident light intensity. The term ϕ_{eq} has been evaluated according to the procedure proposed by Molina et al. [20].

The numerical solution of the proposed model which results in a *2-D* PDE system of equations, is obtained by discretizing the population balance Eq. (10) with finite difference on the mass variable m. The resulting *1-D* PDE system in the z variable is solved by the IMSL subroutine DMOLCH which reduces, through the method of lines, the *1-D* problem to a system of ordinary differential equations (ODEs). The last one is solved using the subroutine DIVPAG of the IMSL libraries.

3. Results and discussion

The reliability of mathematical model is first tested by comparison with the literature experimental data concerning the growth of the cyanobacteria *Spirulina platensis* on "BIOCOIL" photobioreactor [30]. Data by Travieso et al. [30] have been chosen since all the

Table 1
Model parameters used for simulation of Spirulina growth in BIOCOIL photobioreactors.

Parameter	Value	Unit	Reference
K_a	0.15	$m^2\ g^{-1}$	[13]
I_k	160	$\mu E\ m^{-2}\ s^{-1}$	[34]
n	1.49	–	[20]
μ_{max}	2.06×10^{-5}	s^{-1}	[35]
K_{NO_3}	5.314	$g\ m^{-3}$	Calculated from [36].
$K_{H_2PO_4}$	0.028	$g\ m^{-3}$	Calculated from [37]
E_D	6.67×10^{-5}	$m^2\ s^{-1}$	[38]
$C^0_{O_2}$	9.1	$g\ m^{-3}$	Evaluated as reported in the text
$C_{O_{2,max}}$	47.9	$g\ m^{-3}$	[21]
ρ_{cell}	1.02×10^6	$g\ m^{-3}$	[39]
y_{X/NO_3}	2.7	–	[40]
y_{X/H_2PO_4}	40.805	–	Calculated from [41]
y_{X/O_2}	0.534	–	Calculated from [41]
q	40	–	[31]
μ_0	2.6×10^{-10}	g	[42]
σ	1.25×10^{-10}	g	[31]

relevant information for performing the simulations without any adjustable parameter are provided.

S. platensis has been cultivated in a culture medium where all macro-nutrients (N, P) were in concentrations sufficient to sustain the batch microalgal growth for about 1.38×10^6 s (16 days). In particular Na_2CO_3 was present in the medium at high concentrations so that no limitations due to carbon depletion may take place. In addition, the continuous supply of air enriched with CO_2 (4%) in the airlift avoided any carbon limitation during the process. The BIOCOIL photobioreactor has a cylindrical shape (0.9 m height) with a 0.25 m^2 basal area and a photostage comprising 60 m of transparent PVC tubing having 0.016 m of inner diameter. The inner surface of the cylinder was illuminated with fluorescent lamps which guaranteed an incident light intensity of about 70.15 $\mu E\ m^{-2}\ s^{-1}$ for the first 9×10^5 s (10 days). Subsequently a light intensity of 156.64 $\mu E\ m^{-2}\ s^{-1}$ was used [30].

The flow-rate v_z inside the tube was equal to 0.19 $m\ s^{-1}$ [30]. The remaining model parameters, whose values are reported in Table 1, are taken from the literature related to either the original work from which the experimental data have been taken or to specific sources where other model parameters values were available.

All the parameters used in the simulation are related to microalga *S. platensis*. Only the coefficient n, the maximum allowed O_2 concentration ($C_{O_2,max}$) is related to different types of microalgae due to the lack of the corresponding values in the literature. As for as the yields of nutrients $y_{X/j}$, their values are obtained by the average stoichiometry for *S. platensis* proposed by Paille et al. [41]. The initial mass distribution of cells was calculated by considering that typical *S. platensis* tricomes are constituted by a sequence of cylindrical shaped cells having diameter ranging from 4×10^{-6} to 12×10^{-6} m with an average value of 8×10^{-6} m. The cell length varies from 2×10^{-6} to 3×10^{-6} m with an average value of 2.5×10^{-6} m [33]. By considering a specific mass of the single cell of $1.02 \times 10^6\ g\ m^{-3}$, an average cell mass value of 1.28×10^{-10} g was calculated along with its standard deviation. The initial mass distribution was assumed to be of Gaussian type and was evaluated through Eq. (16) to obtain the total initial biomass concentration of 250 $g\ m^{-3}$ as reported in the literature [30]. As for as the other parameters, the average mass of dividing cells, μ_0, appearing in Eq. (14), is assumed equal to about twice the value of the mode of the initial distribution (i.e. 2.6×10^{-10} g). This seems a reasonable choice as suggested by Pisu et al. [42]. Regarding the other parameters related to the division probability density and partitioning functions, i.e. σ and q, respectively, we select typical values for mass structured cell population balance models in an environment of changing substrate concentrations [31]. In Fig. 2, model predictions,

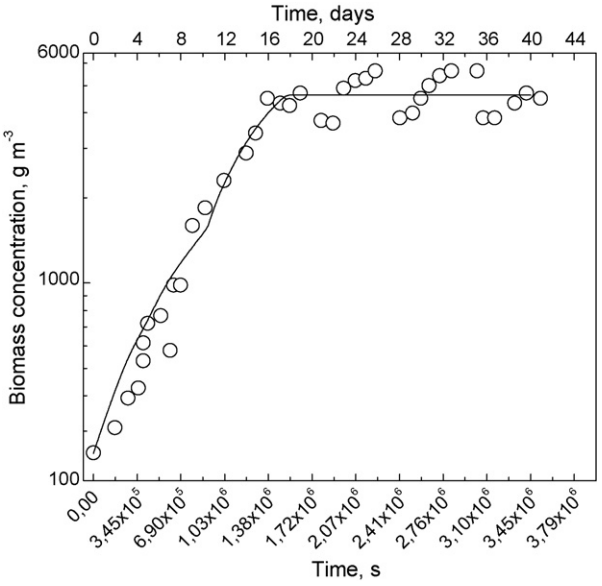

Fig. 2. Biomass concentration growth in the final section of the tube (log scale) as predicted by the proposed model (continuous line) and comparison with the literature [30] data (○).

in terms of biomass concentration as a function of time at the final section of the tube, are compared with the experimental data by Travieso et al. [30]. While it is seen that the matching is quite good, thus demonstrating the reliability of the proposed model as well as its predictive capability, the latter one does not properly simulate the scattered experimental data after 1.81×10^6 s (about 21 days), of culture are reached. This is because, once the stationary phase is reached during experiments, the photobioreactor was operated in a semi-continuous mode by stepwise replacement of its medium using suitable solutions [30]. Since this experimental operation is not accounted for in the present model, a good matching with experimental data cannot be obtained with respect to the entire range of the available experimental data. However, the proposed model is able to quantitatively simulate the obtained experimental data even under the semi-continuous mode described above since the stepwise replacement of the medium involves a relatively small percentage of the liquid volume circulating within the reactor so that the corresponding steady state behavior resulted to be anyway well interpreted by the model.

It is worth noting that the change in the slope of model results at $t = 9 \times 10^5$ s (10 days) is related to the light intensity increase from 70.15 to 156.64 $\mu E\ m^{-2}\ s^{-1}$ performed during the experiment, which as expected, affects microalgal growth kinetics. The photosynthetically active radiation within the culture in the final section of the tube is also shown in Fig. 3. It is seen that while at the early stage of algae culture the difference between the incident radiation and the corresponding active one is relatively small, it significantly increases as the biomass grows.

Fig. 4 illustrates the calculated nutrient and oxygen concentrations as a function of time in the final section of the tube ($z = L$). Unfortunately, model results cannot be compared with experimental data since the latter ones were not available [30].

From Fig. 4 it is possible to observe that at about 1.55×10^6 s (18 days) of algae culture the total consumption of nutrient NO_3^- in the culture medium is reached. Under these conditions, the photosynthetic activity is stopped, as demonstrated by the oxygen concentration which reaches the value of $C^0_{O_2}$ corresponding to that one at the degasser exit. In the simulation, this value has been set equal to the saturation concentration of oxygen in water at 25 °C (9.1 $g\ m^{-3}$). It is also apparent that while the time profile of the

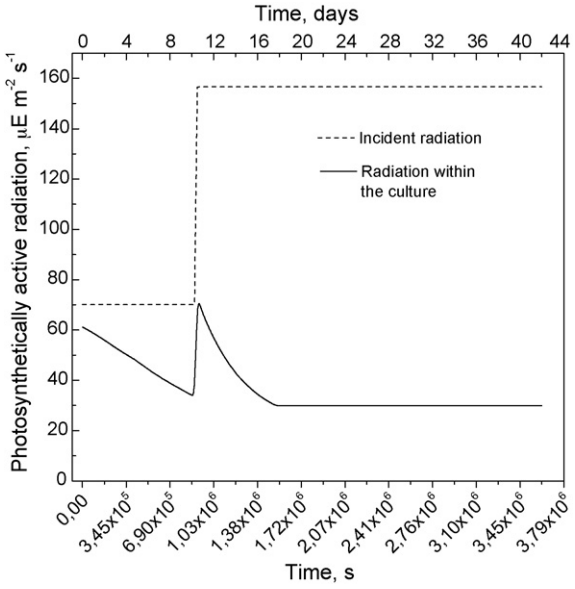

Fig. 3. Time evolution of photosynthetically active radiation in the final section of the tube as predicted by the proposed model (continuous line) is compared with the incident radiation values (dotted line).

nutrient $H_2PO_4^-$ is similar to that one of NO_3^-, although it did not drop to zero, oxygen concentration within the culture first increases at different rates depending upon both the augmentation of the incident radiation and the algae metabolism which represents an oxygen source. It then reaches a maximum at about 1.12×10^6 (13 days) and then start decreasing as the concentration of the nutrients drops below certain values, according to the time rate of change of cell mass given in Eq. (9) and the way the reactor is operated, i.e. produced oxygen is removed at the degasser.

Since the inhibitory action of O_2 plays a crucial role in the scaling-up of this technology, in Fig. 5 the axial profiles of O_2 concentration along the tube are reported for different times.

From the same figure it is possible to observe that the oxygen concentration within the liquid phase keeps increasing inside the photobioreactor since the biomass, whose metabolism produces oxygen, constantly increases. However, as observed above, the concentration levels keeps decreasing after the corresponding maximum values are reached, as the culture time is augmented.

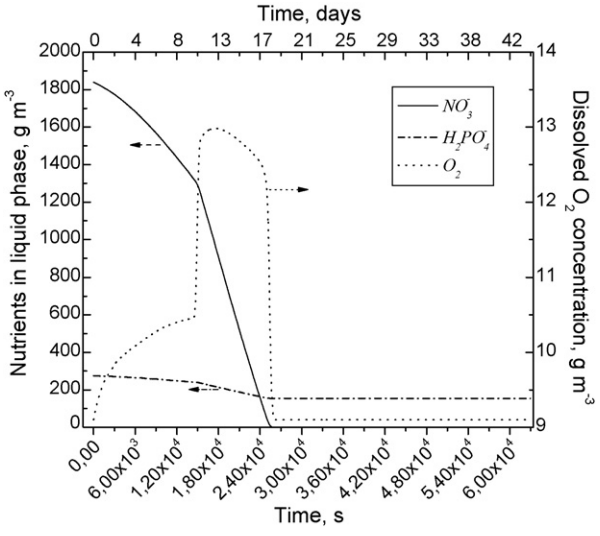

Fig. 4. Time evolution of nutrients and oxygen concentrations in the final section of the tube, as predicted by the proposed model.

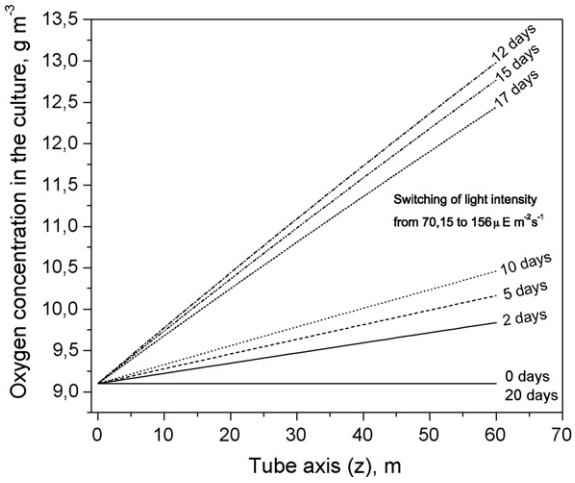

Fig. 5. Oxygen concentration along the tube axis (z) as predicted by the proposed model.

The time evolution of the cell mass distribution in the final section of the tube is reported in Fig. 6. It is possible to observe that cell distribution displays a typical transient behavior, thus moving back and forth as mitosis and growth phenomena take place. Starting from an unimodal population (with mode 1.28×10^{-10} g), cell proliferation begins. Subsequently, cells gain weight to reach their mitotic size which is close to the value of μ_0. After 2.16×10^5 to 2.59×10^5 s, the distribution becomes bimodal with modes that correspond to peaks of mother and daughter cells. Then, the distribution becomes once again unimodal with an average cell mass different from the starting one. This behavior is described by the mass structured population balance proposed in the present work. In particular, from the analysis of the cell population distribution it is possible to extrapolate the temporal evolution of the average cell mass which displays an oscillating behavior as shown in Fig. 7. This fact may be explained considering that the average mass of dividing cells (μ_0) has been set equal to a value slightly greater than twice of the average cell mass of the initial cell distribution (ψ^0), so that a certain time is required for cells to gain mass and reach the mitotic condition. After cell mitosis, the average cell mass decreases (daughter cells are smaller than the mother ones). Then, cells keep on growing to reach mitotic condition and the average cell mass increases again. During the cultivation time the amplitude

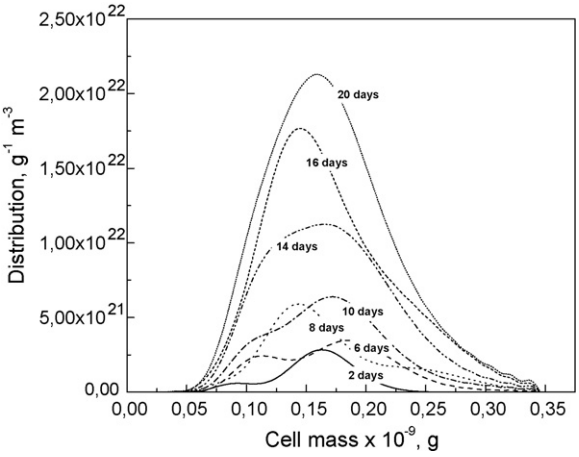

Fig. 6. Cell distribution in the final section of the tube as predicted by the proposed model.

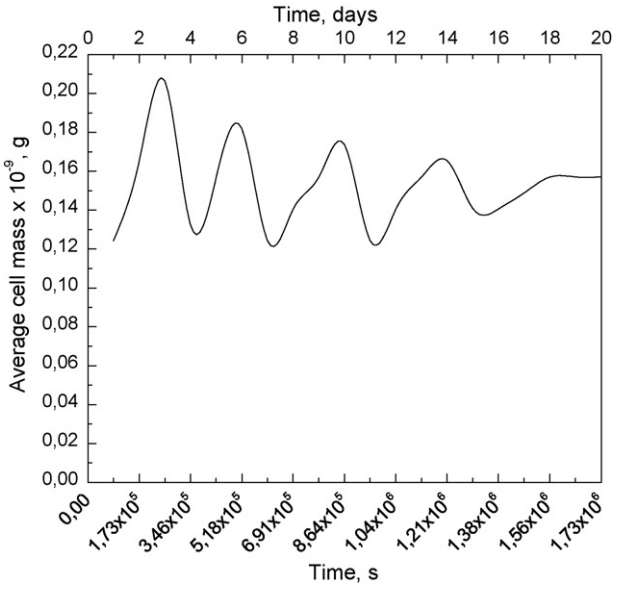

Fig. 7. Mean cell mass evolution in the final section of the tube as predicted by the proposed model.

of oscillations decrease and the average cell mass remain stable around the value of 1.57×10^{-10} g, since the photosynthetic activity stops due to the complete consumption of nutrients. Although for the algae used during experimental runs it would be more useful to know the mass of thricomes rather than that one of single cell, as for the case of unicellular microalgae, i.e. chlorella, haematococcus, etc., the evolution of the cell population distribution may be particularly helpful when a specific cell mass (size) is desired so that the corresponding harvesting operations may be optimized.

4. Conclusions

The mathematical simulation of microalgal growth in the solar collector of BIOCOIL photobioreactors is addressed in this work. The model, which simulates temporal evolution of cells, macronutrient and oxygen concentration in liquid medium along the tube, by taking advantage of mass structured population balance is able to quantitatively describe the cell mass distribution during the process. By comparing model results with the literature experimental data a good matching is obtained thus confirming the capability of the population balance approach when describing cell growth and its proliferation. A possible future direction of this work may take into account the description of the interphase mass transfer of O_2 and CO_2 in the liquid phase along with the related chemical equilibria which may influence the sequestration process. Also modeling of interphase mass transfer phenomena occurring in the airlift will be addressed in future works.

5. Notations

C_j	concentration of jth nutrient in culture medium ($g\,m^{-3}$)
C_{O_2}	dissolved oxygen concentration in culture medium ($g\,m^{-3}$)
$C_{O_2,}$	dissolved oxygen concentration at which algal growth is inhibited ($g\,m^{-3}$)
E_D	axial dispersion coefficient ($m^2\,s^{-1}$)
I	photosynthetically active radiation within the culture ($\mu E\,m^{-2}\,s^{-1}$)
I_0	incident photosynthetically active radiation ($\mu E\,m^{-2}\,s^{-1}$)
I_k	half saturation constant for photosynthetically active radiation ($\mu E\,m^{-2}\,s^{-1}$)
K_a	optical extinction coefficient ($m^2\,g^{-1}$)
K_j	half saturation constant of jth nutrient ($g\,m^{-3}$)
L	reactor length (m)
m	single cell mass (g)
n	coefficient appearing in the rate of cell growth
p	partitioning function (g^{-1})
q	coefficient appearing in the beta function
t	time (s)
X	biomass concentration ($g\,m^{-3}$)
$y_{X/j}$	ratio of weight of dry biomass produced to weight of jth nutrient consumed
y_{X/O_2}	ratio of weight of dry biomass produced to weight of oxygen produced
v_z	fluid velocity ($m\,s^{-1}$)
z	spatial coordinate (m)

Greek letters

$\beta(q,q)$	symmetric beta function
Γ	division rate function (s^{-1})
μ_0	average mass of dividing cells (g)
μ_{max}	maximum specific rate of cell growth (s^{-1})
μ_c	catabolic growth rate (s^{-1})
ζ_m	time rate of change of cell mass m ($g\,s^{-1}$)
ϕ_{eq}	average length of light path (m)
σ	standard deviation of the Gaussian distribution
ψ	cell distribution function in a generic spatial position ($g^{-1}\,m^{-3}$)

Superscripts

0	initial conditions
$'$	mother cell

Subscripts

j	nutrient
O_2	oxygen

Acknowledgements

This work is carried out with the financial contribution of the Sardinian Regional Authorities. The financial support of BT (Biomedical Tissues) Srl, Italy, is also gratefully acknowledged.

References

[1] Y. Chisti, Biodiesel from microalgae, Biotechnol. Adv. 25 (2007) 294–306.
[2] Y. Chisti, Biodiesel from microalgae beats bioethanol, Trends Biotechnol. 26 (2008) 126–131.
[3] Y.K. Lee, Enclosed bioreactors for the mass cultivation of photosynthetic microorganisms: the future trend, Trends Biotechnol. 4 (1986) 186–189.
[4] M.R. Tredici, R. Materassi, From open ponds to vertical alveolar panels: the Italian experience in the development of reactors for the mass cultivation of phototrophic microorganisms, J. Appl. Phycol. 4 (1992) 221–231.
[5] O. Pulz, Photobioreactors: production systems for phototrophic microorganisms, Appl. Microbiol. Biot. 57 (2001) 287–293.
[6] E. Molina Grima, F. García Camacho, J.A. Sanchez Perez, J. Fernandez Sevilla, F.G. Acién Fernández, A. Contreras Gomez, A mathematical model of microalgal growth in light limited chemostat cultures, J. Chem. Technol. Biotechnol. 61 (1994) 167–173.
[7] Y. Watanabe, J. de la Noue, D.O. Hall, Photosynthetic performance of a helical tubular photobioreactor incorporating the cyanobacterium *Spirulina platensis*, Biotechnol. Bioeng. 47 (1995) 261–269.
[8] D.O. Hall, F.G. Acién Fernández, E. Cañizares, K. Rao, E. Molina Grima, Outdoor helical tubular photobioreactors for microalgal production: modelling of fluid-dynamics and mass transfer and assessment of biomass productivity, Biotechnol. Bioeng. 82 (2003) 62–73.
[9] J. Doucha, K. Livansky, Novel outdoor thin-layer high density microalgal culture system: productivity and operational parameters, Algol. Stud. 76 (1995) 129–147.

[10] M.R. Tredici, P. Carlozzi, G. Chini, R. Materassi, A vertical alveolar panel for outdoor mass cultivation of microalgae and cyanobacteria, Bioresour. Technol. 38 (1991) 153–159.
[11] E. Sierra, F.G. Acién Fernández, J.M. Fernández, J.L. García, C. González, E. Molina Grima, Characterization of a flat plate photobioreactor for the production of microalgae, Chem. Eng. J. 138 (2008) 136–147.
[12] E. Waltz, Biotech's green gold? Nat. Biotechnol. 27 (2009) 15–18.
[13] J.F. Cornet, C.G. Dussap, J.B. Gros, C. Binois, C. Lasseur, A simplified monodimensional approach for modeling coupling between radiant light transfer and growth kinetics in photobioreactors, Chem. Eng. Sci. 50 (1995) 1489–1500.
[14] F.G. Acién Fernández, F.G. García Camacho, J.A. Sanchez-Perez, J.M. Fernandez Sevilla, E. Molina Grima, A model for light distribution and average solar irradiance inside outdoor tubular photobioreactors for the microalgal mass culture, Biotechnol. Bioeng. 55 (1997) 701–714.
[15] C. Zonneveld, H.A. van den Berg, S.A.L.M. Kooijman, Modeling carbon cell quota in light-limited phytoplankton, J. Theor. Biol. 188 (1997) 215–226.
[16] E. Molina Grima, F.G. Acién Fernández, F. García Camacho, Y. Chisti, Photobioreactors: light regime, mass transfer, and scaleup, J. Biotechnol. 70 (1999) 231–247.
[17] G.L. Rorrer, R.K. Mullikin, Modeling and simulation of a tubular recycle photobioreactor for macroalgal cell suspension cultures, Chem. Eng. Sci. 54 (1999) 3153–3162.
[18] F. Camacho Rubio, F.G. Acién Fernández, J.A. Sanchez Perez, F. García Camacho, E. Molina Grima, Prediction of dissolved oxygen and carbon dioxide concentration profiles in tubular photobioreactors for microalgal culture, Biotechnol. Bioeng. 62 (1999) 71–86.
[19] X. Wu, J.C. Merchuk, A model integrating fluid dynamics in the photosynthesis and photoinhibition process, Chem. Eng. Sci. 56 (2001) 3527–3538.
[20] E. Molina Grima, J. Fernandez Sevilla, F.G. Acién Fernández, Y. Chisti, Tubular photobioreactor design for algal cultures, J. Biotechnol. 92 (2001) 113–135.
[21] J. Li, N.S. Xu, W.W. Su, Online estimation of stirred-tank microalgal photobioreactor cultures based on dissolved oxygen measurement, Biochem. Eng. J. 14 (2003) 51–65.
[22] M. Berenguel, F. Rodrıguez, F.G. Acién Fernández, J.L. Garcıa, Model predictive control of pH in tubular photobioreactors, J. Process. Contr. 14 (2004) 377–387.
[23] J. Pruvost, J.F. Cornet, J. Legrand, Hydrodynamics influence on light conversion in photobioreactors: an energetically consistent analysis, Chem. Eng. Sci. 63 (2008) 3679–3694.
[24] P.H.C. Eilers, J.H.C. Peeters, A model for the relationship between light intensity and the rate of photosynthesis in phytoplankton, Ecol. Model. 42 (1988) 199–215.
[25] K. Banse, Rates of growth, respiration and photosynthesis of unicellular algae as related to cell size—a review, J. Phycol. 12 (1976) 135–140.
[26] R.J. Geider, T. Platt, J.A. Raven, Size dependence of growth and photosynthesis in diatoms: a synthesis, Mar. Ecol. Prog. Ser. 30 (1986) 93–104.
[27] R.J. Yang, X.L. Wang, Y.Y. Zhang, Y.J. Zhan, Influence of cell equivalent spherical diameter on the growth rate and cell density of marine phytoplankton, J. Exp. Mar. Biol. Ecol. 331 (2006) 33–40.
[28] M. Hein, M.P. Foldager, K. Sand-Jensen, Size-dependent nitrogen uptake in micro- and macroalgae, Mar. Ecol. Prog. Ser. 118 (1995) 247–253.
[29] J. Horiuchi, I. Ohba, K. Tada, M. Kobayashi, T. Kanno, M. Kishimoto, Effective cell harvesting of the halotolerant microalga Dunaliella tertiolecta with pH control, J. Biosci. Bioeng. 95 (2003) 412–415.
[30] L. Travieso, D.O. Hall, K.K. Rao, F. Benítez, E. Sánchez, R. Borja, A helical tubular photobioreactor producing Spirulina in a semicontinuous mode, Int. Biodeter. Biodegr. 47 (2001) 151–155.
[31] N.V. Mantzaris, J.J. Liou, P. Daoutidis, F. Srienc, Numerical solution of a mass structured cell population balance in an environment of changing substrate concentration, J. Biotechnol. 71 (1999) 157–174.
[32] J.T. Lehman, D.B. Botkin, G.E. Likens, The assumptions and rationales of a computer model of phytoplankton population dynamics, Limnol. Oceanogr. 20 (1975) 343–364.
[33] D.M. Himmelblau, K.B. Bischoff, Process Analysis and Simulation: Deterministic Systems, Wiley, New York, 1968.
[34] A. Vonshak, *Spirulina platensis* (Arthrospira). Physiology, Cell-Biology and Biotechnology, Taylor & Francis, London, UK, 1997.
[35] E. Kebede, G. Ahlgren, Optimum growth conditions and light utilization efficiency of *Spirulina platensis* (=Arthrospira fusiformis) (Cyanophyta) from Lake Chitu, Ethiopia, Hydrobiologia 332 (1996), 99–109.
[36] S.F. Baldia, T. Nishijima, Y. Hata, Growth characteristics of a blue green alga *Spirulina platensis* for nitrogen utilization, Nippon Suisan Gakk. 57 (1991) 645–654.
[37] S.F. Baldia, T. Nishijima, Y. Hata, Effects of physico-chemical factors and nutrients on the growth of *Spirulina platensis* isolated from Lake Kojima, Japan, Nippon Suisan Gakk. 57 (1991) 481–491.
[38] F. Camacho Rubio, A. Sánchez Mirón, M.C. Cerón García, F. García Camacho, E. Molina Grima, Y. Chisti, Mixing in bubble columns: a new approach for characterizing dispersion coefficients, Chem. Eng. Sci. 59 (2004) 4369–4376.
[39] T.J. Smayda, J. Boleyn, Experimental observations on the flotation of marine diatoms. I. Thalassiora cf. nana, Thalassiora rotula, and Nitzschia seriata, Limnol. Oceanogr. 10 (1965) 499–510.
[40] E.D.G. Danesi, C.O. Rangel-Yagui, J.C.M. Carvalho, S. Sato, Effect of reducing the light intensity on the growth and production of chlorophyll by *Spirulina platensis*, Biomass Bioenergy 26 (2004) 329–335.
[41] C. Paille, J. Albiol, R. Curwy, C. Lasseur, F. Godia, FEMME: a precursor experiment for the evaluation of bioregenerative life support systems, Planet. Space Sci. 48 (2000) 515–521.
[42] M. Pisu, A. Concas, G. Cao, A novel simulation model for stem cells differentiation, J. Biotechnol. 130 (2007) 171–182.